SLAC–PUB–5599
UCD–91–10
July 1991
(M)

ISOLATING PURELY LEPTONIC SIGNALS FOR STRONG W SCATTERING USING ANTI-TAGGING, JET-TAGGING AND LEPTON ISOLATION*

D. A. DICUS
Center for Particle Theory,
University of Texas at Austin, Austin, TX 78712

J. F. GUNION AND L. H. ORR
Department of Physics,
University of California, Davis, CA 95616

R. VEGA
Stanford Linear Accelerator Center,
Stanford University, Stanford, CA 94305

Submitted to *Nuclear Physics B.*

* Work supported by Department of Energy contracts DE–AC03–76SF00515, DE–FG05–85ER40200, and DE–AT03–89ER40492.

Abstract

We explore in depth several techniques for detecting the l^+l^+ mass spectrum coming from W^+W^+ scattering at a hadron collider. We focus on the signal, due to enhanced production of longitudinally polarized W^+'s, that arises in the Standard Model when the Higgs boson has mass $\gtrsim 1$ TeV. We demonstrate that anti-tagging against energetic centrally produced jets must be combined either with our earlier-proposed cut (requiring single-jet tagging) on the minimum jet-lepton invariant mass or with a cut on the isolation of the leptons in order to adequately suppress all backgrounds. In particular, we identify cuts that are sufficient to suppress the $t\bar{t}$-induced backgrounds below the level of the signal. Effects due to production of an extra gluon in association with the $t\bar{t}$ are included. Sensitivity to distribution functions and scale choices is explored. Event rates at the LHC, SSC and Eloisatron energies are given. Use of the isolation requirement along with staged implementation of the other cuts is proposed as a means for verifying the Standard Model expectation for the W^+W^+ spectrum in the case where the Higgs boson is light. Applicability of the proposed cut procedures to the purely leptonic decay modes of the W^+W^-, ZZ and $W^\pm Z$ channels is outlined.

1. Introduction

The importance of the like-sign dilepton spectrum as a means of detecting strong scattering of *longitudinally* polarized W^+'s has been frequently discussed, as has the necessity of overcoming the background from production of transversely polarized W^+'s.[1-3] Efficient techniques for suppressing the transverse polarization background were established in Refs. [4] and [5], and complementary work has recently appeared in Ref. [6]. In particular, in Refs. [4] and [5] it was found that anti-tagging against energetic jets produced in association with the like-sign leptons was very effective in discriminating against events containing transversely polarized W^+'s in the final state, while at the same time allowing retention of most events in which both W^+'s are produced with longitudinal polarization. Altogether, these techniques allow observation of a longitudinal polarization signal larger than or comparable in magnitude to that predicted in the SM computation in the case of $m_{\phi^0} = 1$ TeV, provided the only background is that from events in which one or both of the W^+'s are transversely polarized.

However, in Ref. [5] it was found that additional cuts are needed in order to adequately suppress the background from $t\bar{t}$ production events in which one obtains like-sign leptons from the chain $t \to bW^+$, $W^+ \to l^+\nu$, and $\bar{t} \to \bar{b}\, jets$, $\bar{b} \to \bar{c}\, l^+\nu$.[⋆] One possible procedure involving the tagging of a single jet was developed in Ref. [5]. Here, we explore in greater depth this technique, including $t\bar{t}g$ final states, and also a possible alternative employing a requirement of lepton isolation. Our conclusion is that either of the procedures we shall discuss will almost certainly enable one to severely suppress the $t\bar{t}$-induced backgrounds while retaining the bulk of the events in which longitudinally polarized W^+'s are produced. We also include a discussion of the sensitivity of background and signal event rates to distribution function and renormalization scale choices, as well as event rate dependence on machine energy. We conclude with remarks on the utility of our cuts for confirming Standard Model expectations for the W^+W^+ spectrum if the Higgs boson is light, and for detecting the longitudinal-polarization signal in the purely leptonic decay modes of the W^+W^-, ZZ, and $W^\pm Z$ final states.

2. Definition of the Signal

Before proceeding, it is important to define more exactly what constitutes the signal for strong W^+W^+ scattering. Since strong interactions in the EWSB sector (due, *e.g.*, to a large Higgs boson mass, $\gtrsim 1$ TeV) are the primary source of events in which *both* gauge bosons in the final state are longitudinally polarized, the ideal would be to simply isolate the cross section for the production of longitudinally polarized W^+'s. However, in the $l^+\nu l^+\nu$ final state, an experimental extraction of

⋆ We have also examined the alternate case where the anti-top decays instead via $\bar{t} \to \bar{b}\, l^-\bar{\nu}$. We find that the cuts we discuss, combined with the high probability for observing the l^-, make this final state channel of the $t\bar{t}$ background completely negligible.

the separate polarizations of the final state W^+'s is not actually possible. The only truly observable cross section is that deriving from the sum over all polarizations at the matrix element level. Thus, the only experimentally meaningful procedure is to define the 'signal' (S) as the difference between the full cross section computed for $m_{\phi^0} = 1$ TeV and that computed for $m_{\phi^0} = 50$ GeV. In other words, the signal is defined as the *excess* cross section which arises from choosing a large Higgs mass compared to that predicted for a small Higgs mass. The $m_{\phi^0} = 50$ GeV cross section will be termed the 'background' (B). In our notation, B includes only the $\mathcal{O}(\alpha^2_{\mathbf{weak}})$ diagrams; the contributions from gluon exchange diagrams will be given separately, and are independent of Higgs mass.

It is useful to discuss more explicitly how S and B are related to the cross sections for production of transversely and longitudinally polarized W^+'s. In the past (in particular in Ref. [5]), we have casually and somewhat incorrectly denoted the low-Higgs-mass cross section as $\sigma(TT)$, T referring to transverse polarizations. In fact, there are two things wrong with this notation. First, this notation implies that the density matrix is diagonal, something that is only true if azimuthal angles for the W^+ decay products are integrated over. When strong cuts are imposed on the leptons into which the W^+'s decay, azimuthal angle integrals tend to be rather incomplete; we have verified that off-diagonal terms in the density matrix become significant for the cuts we employ. Second, it is not true that the cross section at low Higgs mass derives entirely from transverse modes. This is most easily discussed using cuts ('theorists cuts' in the language of Ref. [6]) on the W^+'s, and not on the leptons into which they decay; for such cuts, the azimuthal integrals are complete and diagonal notation is appropriate. If cuts are imposed on the outgoing W^+'s requiring them to have large W^+W^+ pair invariant mass and small rapidity, the LT modes are suppressed relative to the TT modes at all Higgs masses, but they cannot be neglected.† Not surprisingly, therefore, when cuts are imposed on the directly observable leptons, rather than on the W^+'s, we find that diagonal and off-diagonal density matrix LT combinations are not entirely insignificant. However, within the accuracy of our computations we have found that they *are* independent of Higgs mass. In particular, if we compute the theoretically definable cross section obtained when only L polarizations are allowed for the two final W^+'s, $\sigma(LL)$, we find that $\sigma(S) \simeq \sigma(LL)$ for all choices of cuts. Thus, the LL polarization component provides the bulk of the signal cross section, and it will be useful to plot distributions for just the LL component in illustrating contrasts to those for the light-Higgs-mass background.

3. SSC Results

† Of course, in the extreme where no cuts on the W^+'s are imposed, LT modes become very important; for instance, at $m_{\phi^0} = 50$ GeV slightly more than half of the uncut W^+W^+ pair cross section derives from LT final state polarization combinations. (Both these observations are in agreement with the results of Refs. [4] and [6].)

Numerical results in this section will be presented for the SSC energy of $\sqrt{s} =$ 40 TeV. We used $\alpha = 1/128$ and $\sin^2\theta_W = 0.22$. Results are insensitive to the precise values chosen for m_W and m_Z; we used the values given by the above $\sin^2\theta_W$ choice. For the quark and gluon distributions our 'standard' choice will be the BCDMS fit of the HMRS collaboration (HMRS(B)).[7] The HMRS(B) fit yields $\Lambda_{\overline{MS}} = 0.19$ GeV (4 flavors); for consistency, we used this same $\Lambda_{\overline{MS}}$ value in evaluating the running strong coupling constant. The best choice of scale at which to evaluate the distribution functions and g_s can only be determined when higher order correction calculations are available. In Ref. [6] it is argued that, for the true W^+W^+ signal and background, momentum scales of order m_W are appropriate. In particular, they employ the scale

$$Q^2 = \tfrac{1}{2}(p_{T\,j_1}^2 + p_{T\,j_2}^2) + m_W^2. \tag{1}$$

In this paper, for most of our results we choose to compute all reactions using momentum transfer equal to the subprocess energy scale, $Q^2 = \hat{s}$. This latter is a conservative choice in that it enhances the $t\bar{t}$ backgrounds, proportional to the gg distribution function luminosity, relative to the signal, which is proportional to the qq and $q\bar{q}$ luminosities. However, for subprocess energies above 1 TeV, the HMRS(B) distribution function program uses the distributions obtained at 1 TeV. Since a large percentage of our cross sections correspond to such subprocess energies, in practice our programs do not fully implement the conservative momentum transfer scale.

Later in this paper, we will explore, to some extent, the sensitivity to the above choices. In particular, we shall compare the HMRS(B) results to those obtained for the updated EHLQ set[8] for both $Q^2 = \hat{s}$ and Q^2 as in Eq. (1). We shall see that all these combinations lead to signal and background cross sections that are fairly similar to those to be presented in this section for HMRS(B) and $Q^2 = \hat{s}$. For the $Q^2 = \hat{s}$ choice, we expect that higher order corrections to the subprocesses involved in our calculations will be positive, but they probably do not exceed 30-40%.

Other points in our analysis to note include the following. Final state parton jets are coalesced when they are separated by $\Delta R < 0.5$, prior to performing the cuts involving jets to be discussed below. Except where noted, our computations for the $t\bar{t}$ and $t\bar{t}g$ backgrounds employ $m_t = 200$ GeV. This choice was made since, for the tagged jet cut to be discussed later, the top-induced backgrounds are largest for large m_t, and since $m_t = 200$ GeV is near the upper limit allowed by the experimental limit of $\Delta\rho \lesssim 0.01$ for corrections to the Standard Model tree-level result of $\rho = m_W^2/(m_Z^2\cos^2\theta_W) = 1$.[9] Sensitivity to m_t will be discussed where appropriate. Finally, it turns out that, for the cuts we employ, the $t\bar{t}$-induced backgrounds are very sensitive to the precise b and c quark masses employed.

The bulk of our numerical results are for $m_b = 5.2$ GeV and $m_c = 1.5$ GeV. This first choice is conservative in the sense that the lepton spectrum from $\bar{b} \to \bar{c}\nu l^+$ decay is fairly hard and the $t\bar{t}$ backgrounds pass the lepton cuts discussed below

with comparative ease. Alternative choices for m_b and m_c can be obtained from a fit[10] to CLEO data for B decay lepton spectra using the model of Altarelli *et al.*.[11] In this model, a B meson decays by first splitting into a spectator quark and a free b quark, which then decays semileptonically. The invariant mass of the decaying b quark is determined by the B mass and the spectator quark momentum (assumed to have a gaussian distribution, with width given by $\sigma = P_F/\sqrt{2}$). Fits to the lepton spectrum from CLEO data[10] yield $m_c = 1680 \pm 80 \pm 40$ MeV and $P_F = 300 \pm 70 \pm 40$ MeV. We have incorporated these results into our analysis by subtracting P_F from the B meson mass to obtain $m_b = 4.98$ GeV, and by taking $m_c = 1.68$ GeV directly from the fit. The comparisons below indicate that, because of the larger size of m_c/m_b for this fit, the lepton spectrum from b decay is softer and the $t\bar{t}$-induced backgrounds smaller than for our first case choices. Thus, as we shall see below, cuts which successfully reduce the background for our conservative mass choices are more than sufficient if the values used for m_b and m_c are taken from the fit to CLEO data.

Let us review the results of Ref. [5]. The observable parton-level particles for the purely leptonic decay modes of the W^+W^+ pair are the charged leptons (we consider $l = e, \mu$) and the two spectator jets. One detects the presence of a heavy Higgs through an excess of like-sign lepton pairs over a large interval of their pair invariant mass M_{ll} in comparison to the number expected were the Higgs light. As already noted, our standard of comparison will be the number of events expected if $m_{\phi^0} = 50$ GeV. The cuts of Ref. [5] were designed to maximize the enhancement in the M_{ll} spectrum due to a heavy Higgs boson. With regard to the final leptons, in addition to M_{ll} and the transverse momenta magnitudes and rapidities of the individual leptons (p_T^l and y_l respectively), two particularly useful variables were defined:

$$\delta p_T^{ll} = |\vec{p}_T^{\,l_1} - \vec{p}_T^{\,l_2}|, \quad z_{ll} = \hat{p}_T^{\,l_1} \cdot \hat{p}_T^{\,l_2} . \tag{2}$$

In events for which $|y_l| < 3.5$ for both leptons, the scattering of longitudinally polarized vector bosons tends to produce events where the p_T^l's are large, where the two leptons are nearly back to back (z_{ll} near -1), and for which δp_T^{ll} is large. In contrast, at low Higgs mass one finds a significant number of events with z_{ll} not near -1 and with small δp_T^{ll} values. An examination of the distributions showed that the following lepton cuts are a good choice for enhancing S/B:

$$M_{ll} > 300 \text{ GeV}, \quad |y_l| < 3.5, \quad p_T^l > 75 \text{ GeV}, \quad z_{ll} < -0.8, \quad \delta p_T^{ll} > 200 \text{ GeV} . \tag{3}$$

The sequential impact of these and other cuts to be discussed shortly is displayed in Table 1. From row 1 and column 1 of Table 1 it follows that the best obtainable rate for the signal (*i.e.* the excess number of events as defined in Sec. 2) is about 12 events per SSC year* in $l^+ = e^+, \mu^+$ channels, and that is before we impose

$\star$ We assume a yearly integrated luminosity of $L = 10\ fb^{-1}$.

any other background suppressing cuts! (In fact lepton charge determination may require a more stringent y_l cut. However, the bottom line rates are not that much affected by this more stringent lepton rapidity cut; see Ref. [5].) As mentioned earlier, to within our Monte Carlo errors, of these 12 events essentially all can be associated with the LL polarization choice. There is no statistically significant indication of an increase with Higgs mass in the sum of diagonal and off-diagonal density matrix terms involving mixed L and T polarizations.

Cut	S	B	g-exch.	$t\bar{t}$	$t\bar{t}g$
$M_{ll} > 300$, $\|y_l\| < 3.5$, $p_T^l > 75$	25	93	29	21000	20000
	(25)	(87)	(20)	(1300)	(210)
$z_{ll} \leq -0.8$, $\delta p_T^{ll} \geq 200$	23	43	13	18000	16600
	(23)	(39)	(7.6)	(950)	(150)
$p_T^{\max,5} \leq 125$	17	7.2	1.4	6800	3970
	(17)	(7.0)	(1.1)	(660)	(82)
$p_T^{\max,5} \leq 125$, $M_{jl}^{\min} \geq 200$	(13)	(3.9)	(.11)	(.85)	(1.7)
$p_T^{\max,5} \leq 125$, $E_{\Delta R=0.25}^{\max} < 8$	17	7.1	1.3	$\sim .03$	$\sim .02$

Table 1: We give the electroweak cross sections in femtobarns for the signal, S, the $\mathcal{O}(\alpha_W^2)$ background, B, as well as those for the $\mathcal{O}(\alpha_W \alpha_s)$ g-exchange background and the $t\bar{t}$ and $t\bar{t}g$ ($m_t, m_b, m_c = 200, 5.2, 1.5$ GeV and $p_T^g \geq 30$ GeV) backgrounds, after imposing various cuts. These latter $t\bar{t}$-induced backgrounds incorporate the branching ratio of 2/3 for $\bar{t} \to \bar{b} jets$. Computations are for the SSC energy of $\sqrt{s} =$ 40 TeV. The B cross section is defined as the SM prediction for $m_{\phi^0} = 50$ GeV, while the S cross section is defined as the excess predicted for $m_{\phi^0} = 1$ TeV compared to the $m_{\phi^0} = 50$ GeV cross section. The lepton cuts of the first row are also imposed in obtaining the second row, and all the lepton cuts of the first two rows are imposed in obtaining all subsequent results. Numbers in parentheses are obtained by requiring that any jet with $|y| < 5$ and $p_T > 30$ GeV be separated by $\Delta R \geq 0.5$ from both l^+'s. The parenthetical $t\bar{t}$ and $t\bar{t}g$ cross sections also include a cut which vetoes events with more than two jets having $p_T > 30$ GeV in $|y| < 5$. All momenta and mass cuts are in GeV units. Branching ratios for the $W^+ \to l^+\nu$ decays are not included. Smearing for the isolation cut employs $A = 0.5$

Turning next to the jets produced in association with the l^+l^+ pair, a number of options will be considered. First, let us define $p_T^{\max,5}$ as the transverse momentum of the associated jet (after coalescence) with largest p_T that lies in the region

$|y| < 5$. (In the case of the W^+W^+ events, there are only two spectator jets to be considered, while for the $t\bar{t}$ and $t\bar{t}g$ backgrounds there are four and five jets in the final state, respectively.) Second, we can consider the number and location of 'observable' energetic jets, defined as jets with $p_T \geq 30$ GeV and $|y| < 5$. We define ΔR_{jl}, the minimum separation between any such energetic jet and either l^+. We also define n_j as the number of such energetic jets. A very effective means for enhancing the longitudinally polarized W^+ cross section contributions was found in Ref. [5] to be anti-tagging via the requirement that $p_T^{\max,5} < 125$ GeV (in addition to the lepton cuts of Eq. (3)). The results of imposing such a cut are given in Table 1. We see that while this additional cut achieves a good S/B ratio, it is still not sufficient to make the S cross section dominant over the $t\bar{t}$ backgrounds. Even requiring that the energetic jets satisfy

$$\Delta R_{jl} \geq 0.5, \quad n_j \leq 2, (\text{when } p_T^j \geq 30, \ |y_j| < 5) \tag{4}$$

(the parenthetical numbers in the table) does not much improve the situation. Thus, we must find additional cuts designed to remove the $t\bar{t}$ backgrounds while retaining the bulk of the signal events.

The Tagged-Jet $M_{jl}^{\rm min}$ Cut Procedure

In ref. [5] the $t\bar{t}$ background was dealt with by explicitly tagging at least one of the spectator jets. The tagging and cut procedure developed there was as follows. Having imposed the lepton cuts of Eq. (3) and the $p_T^{\rm max,5} < 125$ GeV cut, we require that energetic jets obey the cuts of Eq. (4) and that at least one final state jet has $|y| < 5$ and $30 < p_T < 125$ GeV. Such a jet is termed a tagged jet. We compute

$$M_{jl}^{\rm min} = {\rm Min}_{j,l} M_{jl}, \tag{5}$$

where M_{jl} is the invariant mass of a given tagged spectator jet-lepton combination, and the minimization is to be performed over both leptons and over any spectator jet satisfying the tagging criterion. (Because of Eq. (4) no more than two jets can be tagged.) The resulting $M_{jl}^{\rm min}$ distributions are given in Fig. 1.

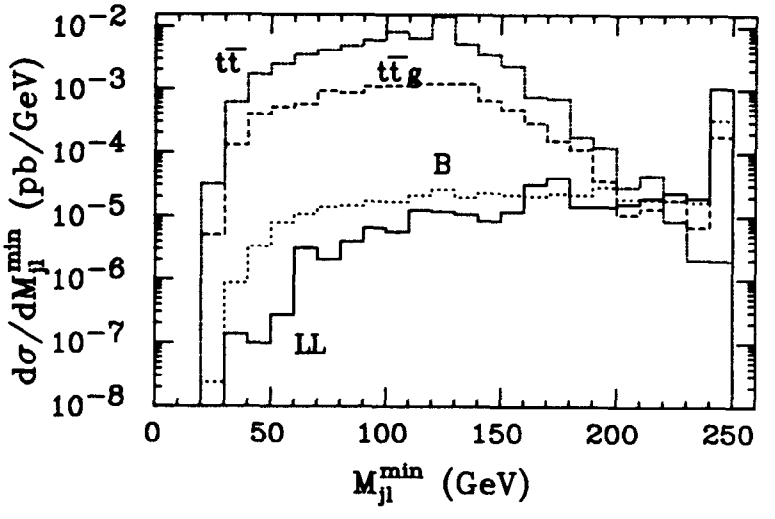

Figure 1: $M_{jl}^{\rm min}$ distributions for the W^+W^+ final state. Results for the $m_{\phi^0} = 50$ GeV B cross section and for the LL cross section computed at $m_{\phi^0} = 1$ TeV are compared. Also illustrated are the distributions from the primary $t\bar{t}$ and $t\bar{t}g$ backgrounds (computed for $m_t = 200$ GeV, $m_b, m_c = 5.2, 1.5$ GeV, and, for $t\bar{t}g$, $p_T^g \geq 30$ GeV). We take $\sqrt{s} = 40$ TeV and employ the cuts of Eqs. (3) and (4) with the added requirement of $p_T^{\rm max,5} < 125$ GeV. Branching fractions for $W^+ \to l^+\nu$ are not included. The $240-250$ GeV bin accumulates all contributions for $M_{jl}^{\rm min} \geq 240$ GeV.

Even though $M_{jl}^{\min}$ is primarily defined to deal with the $t\bar{t}$ background, one also finds a significant difference in the $M_{jl}^{\min}$ distributions for LL (and S) compared to B. The $m_{\phi^0} = 1$ TeV LL mode has substantially larger $M_{jl}^{\min}$ values on average than does the ($m_{\phi^0} = 50$ GeV) B cross section. (This is, of course, due to the fact that LL spectator jets tend to have smaller p_T and especially larger $|y|$ than B spectators, and therefore tend to yield larger jl invariant masses when combined with the high-p_T, small $|y|$ l^+'s.) This is illustrated in Fig. 1. A cut of $M_{jl}^{\min} > 200$ GeV is fairly optimum, yielding the result given in Table 1. (Including $[BR(W^+ \to l^+\nu)]^2 = 4/81$ and multiplying by the expected SSC luminosity, $L = 10\ fb^{-1}$, yields 6.4 S events and 1.9 B events, with an event ratio of $S/B = 3.4$.) The location of this LL/B crossover point is fortunate in that the figure shows that a cut of $M_{jl}^{\min} > 200$ GeV will also eliminate almost all the $t\bar{t}$ background. Indeed, for $m_t < 200$ GeV events with $M_{jl}^{\min} > 200$ GeV arise only as a result of jet coalescence. Before coalescence any jet would have to combine with one or the other l^+ to yield a $M_{jl}^{\min}$ value below m_t. But, even after coalescence, we see that the residual $t\bar{t}$ background is very small, $\lesssim 1\ fb$.

An obvious question, however, arises at this point. Certainly, a substantial number of $t\bar{t}$ events occur in which there is at least one associated relatively hard gluon produced in the final state. Since such a gluon would not come from either t decay, it need not combine with one of the l^+'s to yield $M_{jl}^{\min} < m_t$. Thus, an important question is the extent to which such a final state gluon would destroy the effectiveness of the $M_{jl}^{\min}$ cut. In order to address this issue, we generated $t\bar{t}g$ events (using the exact matrix element of Ref. [12]) in which the gluon is hard enough to pass our basic tagging requirement, *i.e.* we generated events with $p_T^g \geq 30$ GeV. We then subjected these events to precisely the same analysis as discussed above for the signal and $t\bar{t}$ background. The resulting $M_{jl}^{\min}$ distribution is also displayed in Fig. 1. We see that the bulk of the $t\bar{t}g$ distribution is still in the region $M_{jl}^{\min} \leq 200$ GeV. The reason is that most of the final state gluons tend to prefer to be collinear with the t's. Nonetheless, the $M_{jl}^{\min}$ distribution for the $t\bar{t}g$ final state does indeed have a longer tail at high $M_{jl}^{\min}$ than does that for $t\bar{t}$. However, the other cuts, especially the $n_j \leq 2$ cut of Eq. (4), keep the overall level of the cross section sufficiently small. Consequently the $M_{jl}^{\min}$ cut is also effective in removing the $t\bar{t}g$ background; the cross section surviving the $M_{jl}^{\min} > 200$ GeV cut (and preceding cuts) is $\sim 1.7\ fb$. To estimate the $t\bar{t}$-related background we will follow the procedure of simply adding* the $t\bar{t}$ and $t\bar{t}g$ backgrounds computed as above. We find that our net $t\bar{t}$-related background after the $M_{jl}^{\min}$ cut is about 1.3

$\star$ In fact, this will be an overestimate. There is double counting inherent in this procedure that could only be avoided by employing a full order α_s correction scheme which includes the effects of cuts.

events at $L = 10\ fb^{-1}$, compared to the purely electroweak event rates of $S = 6.4$ and $B = 1.9$ events.

Of course, altering the values of the b and c quark masses affects the $M_{jl}^{\min}$ distributions for the $t\bar{t}$ and $t\bar{t}g$ backgrounds. We have compared $m_b, m_c = 5.2, 1.5$ GeV to the choices $m_b, m_c = 4.98, 1.68$ GeV. Keeping $m_t = 200$ GeV we find that the overall normalization of the $M_{jl}^{\min}$ distribution for the $t\bar{t}$ background is roughly a factor of 2.5 smaller for the latter masses, and that the tail at large $M_{jl}^{\min}$ is slightly steeper. The net result is that the cross section for $M_{jl}^{\min} > 200$ GeV is significantly smaller (0.11 fb) than that obtained for the $m_b, m_c = 5.2, 1.5$ GeV case (0.85 fb).

Sensitivity of the $M_{jl}^{\min}$ cut procedure to the top quark mass is also an important question. If the top mass is significantly less than 200 GeV, the $M_{jl}^{\min}$ cut at 200 GeV becomes increasingly effective. For instance, for $m_t = 150$ GeV the $t\bar{t}$ background is larger after imposing just the lepton and $p_T^{\max,5}$ cuts, but we were unable to generate any events that passed the $M_{jl}^{\min} \geq 200$ GeV cut. In the case of the $t\bar{t}g$ background, events with $M_{jl}^{\min} \geq 200$ GeV do occur, but they yield a slightly smaller cross section than in the $m_t = 200$ GeV case. (The increased number of $t\bar{t}g$ events before cuts is compensated by increased difficulty in passing the cuts in such a way that all the entries in the last column of Table 1 are slightly smaller for $m_t = 150$ GeV.) However, should the top quark mass turn out to be significantly larger than 200 GeV, an $M_{jl}^{\min}$ cut threshold of 200 GeV is not necessarily adequate. For instance, if $m_t = 250$ GeV and we follow precisely the previously outlined procedure, we find that the $t\bar{t}$ background yields a cross section of ~ 6.7 femtobarns after requiring $M_{jl}^{\min} \geq 200$ GeV, to be compared with the 0.85 fb appearing in Table 1 (row 4). Raising the cut threshold to 240 GeV reduces the background in this case to below 1 fb, but in so doing ~ 1 fb of the 13 fb signal is sacrificed.

Another question regarding the $M_{jl}^{\min}$ procedure concerns the exact fraction of signal events retained after the $M_{jl}^{\min} \geq 200$ GeV cut. Minimum-bias structure and initial/final state radiated jets in the typical signal event could alter the efficiencies computed here. The exact efficiency can only be established once experiments begin operation at the SSC. In particular, extra gluons radiated in association with W^+W^+ production (in addition to the automatically-present two spectator quark jets) might have sufficient p_T and appropriate $|y|$ to be tagged some significant fraction of the time, and of those tagged some might yield $M_{jl}^{\min}$ values above 200 GeV. Since the two true spectator jets that we wish to single out for the $M_{jl}^{\min}$ procedure generally have large rapidity, and thus very large overall energy, a further cut either on the total jet energy or of the type $|y_j| \geq 3$ (but $|y_j| \leq 5$ still) for the tagged jet(s) might be considered as a means to avoid any tail to the $M_{jl}^{\min}$ distribution from this source. However, this would cause a depletion of the

signal rate. Avoiding this possible problem by raising the p_T^j jet-tagging threshold would also result in some signal rate depletion. We have not pursued either option in this paper.

The Isolation Cut Procedure

Since there are a few possible difficulties associated with the $M_{jl}^{\min}$ cut technique, it is desirable to develop an alternative procedure for eliminating the $t\bar{t}$-induced backgrounds. Such an alternative is potentially provided by focusing on the isolation of the final l^+'s. For each event we compute the amount of *parton* jet energy contained in a cone of size $\Delta R = 0.25$ around each of the final l^+'s. The larger of these two cone energies we denote by $E_{\Delta R=0.25}^{\max}$:

$$E_{\Delta R=0.25}^{\max} = \mathrm{Max}_{l^+}\left\{ \sum_{j;\,\Delta R_{jl^+}<0.25} E_j \right\}. \tag{6}$$

In the case of the W^+W^+ S signal and B background the l^+'s are nearly always isolated from the spectator jets, and the number of events with a non-zero value of $E_{\Delta R=0.25}^{\max}$ is extremely small. In contrast, the collinear nature of $\bar{b} \to \bar{c}\nu l^+$ decay (when p_T^l is required to be large) implies that the $\bar{c}$ will always be quite close to the l^+. In fact, for the $t\bar{t}$ and $t\bar{t}g$ backgrounds all but roughly 0.01% of the cross section has the $\bar{c}$ within $\Delta R = 0.1$ of the l^+, and all events have the $\bar{c}$ within $\Delta R = 0.2$. (Indeed, the only reason for considering a cone as large as $\Delta R = 0.25$ is that hadronization, detector granularity and other such effects are likely to spread the parton-level energy out somewhat. An isolation cone of size 0.25 seems sufficiently conservative to account for such effects.) Since $E_{\Delta R=0.25}^{\max}$ is always $\geq E_{\mathrm{charm}}$, the vast bulk of the $t\bar{t}$ and $t\bar{t}g$ cross sections will come from events with large $E_{\Delta R=0.25}^{\max}$ values. As a result, a requirement that $E_{\Delta R=0.25}^{\max}$ be smaller than some appropriately chosen value is likely to virtually eliminate the $t\bar{t}$ backgrounds while retaining almost all the signal.

There are, however, several complications that must be incorporated into a semi-realistic analysis.[13] First, there are the effects due to bottom quark hadronization, and to decay and hadronization of the charm quark jet. Second, the imperfect detector resolution results in some smearing of the energy deposited in the 0.25 cone. Some of the time the measured energy in the cone will be substantially smaller than that actually deposited. A full assessment of these effects requires a Monte Carlo treatment and is beyond the scope of this paper. We will approximately simulate the combination of such effects by smearing the parton level value of $E_{\Delta R=0.25}^{\max}$ according to a Gaussian distribution with width given by

$$\frac{\Delta E}{E} = \frac{A}{\sqrt{E}} + 0.03\,, \tag{7}$$

where GeV units are employed and the two components of the resolution are to be

added in quadrature. Detector resolution alone would lead to a value of $A = 0.5$.* Our expectation is that the effective value of A that will emerge from a Monte Carlo treatment will lie in the range between 0.5 and 1. We will present results primarily for $A = 0.5$, but $A = 1$ and $A = 2$ will also be considered. Clearly, if the smearing yields a $E^{max}_{\Delta R=0.25}$ distribution that extends to too low a value (*e.g.* of order the energy expected in a $\Delta R = 0.25$ cone from minimum bias, event structure and pileup — estimated to be of order 1.5 GeV on average at $\mathcal{L} = 10^{33}$ cm^{-2} sec^{-1} [15]) then a cut on $E^{max}_{\Delta R=0.25}$ will not be implementable in practice, since a large fraction of the W^+W^+ signal events would also be eliminated.

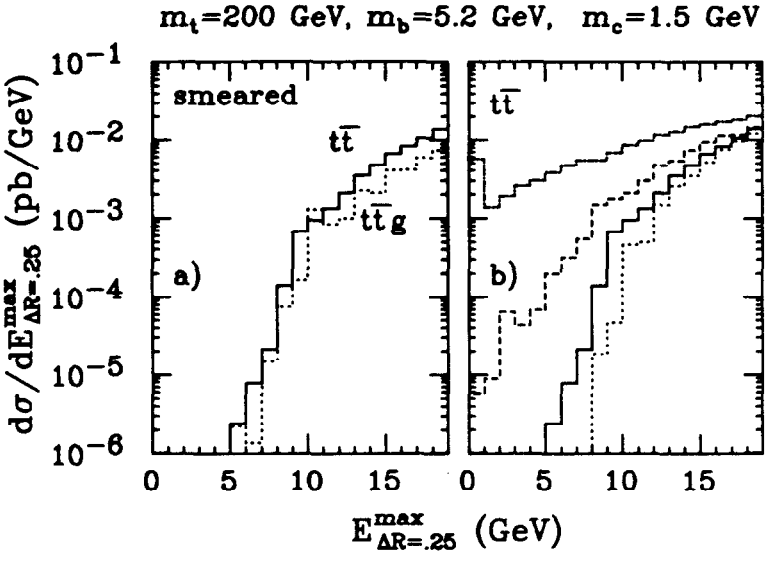

Figure 2: Background $E^{max}_{\Delta R=0.25}$ distributions computed for $m_t = 200$ GeV, $m_b = 5.2$ GeV, and $m_c = 1.5$ GeV. We take $\sqrt{s} = 40$ TeV and employ the cuts of Eqs. (3) with the added requirement of $p_T^{max,5} < 125$ GeV. However, energetic jet cuts and jet tagging are not imposed. Branching fractions for $W^+ \to l^+\nu$ are not included. In a) we compare the $t\bar{t}$ and $t\bar{t}g$ ($p_T^g \geq 30$ GeV) distributions after the hadronic energy in the $\Delta R = 0.25$ cone is smeared using $A = 0.5$ in the resolution of Eq. (7). In b) we compare $t\bar{t}$ results before smearing (dotted), and after smearing with $A = 0.5$ (solid), $A = 1$ (dashed) and $A = 2$ (dot-dashed) effective resolution.

Our quantitative analysis can now be described in detail. We generated signal and background events subject to the lepton cuts of Eq. (3) and the anti-tagging

* Such a resolution is typical of that being considered for SSC detectors; see, for example, the SDC LOI.[14]

$p_T^{\mathrm{max},5} < 125$ GeV cut. The energetic jet cuts of Eq. (4) were *not* imposed in the following lepton isolation analysis, and no specific jet tag was required. For the W^+W^+ S signal and B background, essentially the entire cross section has $E^{\mathrm{max}}_{\Delta R=0.25} \simeq 0$ in our parton level Monte Carlo. Some sample distributions for the $t\bar{t}$-induced backgrounds as a function of the smeared value of $E^{\mathrm{max}}_{\Delta R=0.25}$ are plotted in Fig. 2. In part a) we compare the $t\bar{t}$ and $t\bar{t}g$ $E^{\mathrm{max}}_{\Delta R=0.25}$ distributions after including $A = 0.5$ cone-energy smearing, for the mass choices of $m_t = 200$ GeV, $m_b = 5.2$ GeV, and $m_c = 1.5$ GeV. This comparison exemplifies the typical result that the $t\bar{t}g$ background, generated subject to $p_T^g \geq 30$ GeV, is as easily overcome using lepton isolation as is the $t\bar{t}$ background. Of course, larger cross sections (with very similar shape as a function of $E^{\mathrm{max}}_{\Delta R=0.25}$) result if the p_T^g cutoff is lowered. However, as noted earlier, even for $p_T^g \geq 30$ GeV, simply adding the $t\bar{t}g$ gluon result to that for $t\bar{t}$ is almost certainly double counting to some extent. The $t\bar{t}g$ cross section obtained for $p_T^g \geq 30$ GeV is very similar in size to the $t\bar{t}$ cross section (before any other cuts), and adding the two cross sections together would amount to an effective K factor of order 2, already unreasonably large. In a more rigorous higher order computation, we should subtract from the $t\bar{t}g$ subprocess a (cut-dependent) component which goes into defining the $t\bar{t}$ process at the next order in α_s.

In part b) of Fig. 2 we compare (for the same b and c mass choices) results for the $t\bar{t}$ background before any smearing, and after smearing using $A = 0.5$, $A = 1$ and $A = 2$. From this comparison we see that resolution/hadronization smearing is certainly an important effect, and, if extremely large, could severely limit the effectiveness of an isolation cut. Consider first the optimistic $A = 0.5$ results. Without smearing, an $E^{\mathrm{max}}_{\Delta R=0.25} < 10$ GeV cut would completely eliminate the $t\bar{t}$ and $t\bar{t}g$ backgrounds. After smearing, it is clear that this cut must be reduced to $E^{\mathrm{max}}_{\Delta R=0.25} \lesssim 8$ GeV in order to virtually eliminate these backgrounds. Results for such a cut are given in the bottom row of Table 1.[⋆] We reemphasize that the $t\bar{t}g$ cross section appearing in the table is that obtained for $p_T^g \geq 30$ GeV. Even if we grossly overestimate the $t\bar{t}g$ contribution by lowering the gluon cutoff to $p_T^g \geq 10$ GeV, we still find that the $E^{\mathrm{max}}_{\Delta R=0.25} \leq 8$ GeV cut leaves us with $\lesssim 0.1$ fb of cross section (compared to the 0.02 fb for $p_T^g \geq 30$ GeV).[†] In any case, the 8 GeV cut on $E^{\mathrm{max}}_{\Delta R=0.25}$ is still comfortably above the 1.5 GeV average that one expects to find in a $\Delta R = 0.25$ cone from minimum bias event structure and pile-up. Since at the parton level the S, B and g-exchange process cross sections are confined to very small $E^{\mathrm{max}}_{\Delta R=0.25}$ values, adding minimum bias/pile-up structure to every event

⋆ Increasing the $E^{\mathrm{max}}_{\Delta R=0.25}$ cut to 9 GeV would not actually be a problem, since summing the $t\bar{t}$ and $t\bar{t}g$ cross sections in the $8-9$ GeV bin yields $\lesssim .21$ *fb*.

† Recall that $E^{\mathrm{max}}_{\Delta R=0.25}$ is always greater than or equal to the charm quark energy, so that allowing a softer gluon decreases $E^{\mathrm{max}}_{\Delta R=0.25}$ only to the extent that a softer charm quark distribution results. We have found that altering the gluon cutoff does not greatly alter the momentum distribution of the charm quark.

will not significantly deplete the associated event rates obtained after the $E^{\rm max}_{\Delta R=0.25}$ cut.

Consider now the larger values of $A = 1$ and $A = 2$. If $A = 1$ is an appropriate choice for effectively simulating the net result of the various sources of smearing, Fig. 2 shows that the tail to the $E^{\rm max}_{\Delta R=0.25}$ distribution has much larger cross sections at low $E^{\rm max}_{\Delta R=0.25}$ values. Nonetheless, a cut of $E^{\rm max}_{\Delta R=0.25} \leq 8$ GeV still leaves a net $t\bar{t}$ background cross section of only about 1.3 fb. The $t\bar{t}g$ result is similar, and the net $t\bar{t} + t\bar{t}g$ background remains comfortably below the signal level of 17 fb given in Table 1. However, should $A = 2$ be appropriate there is no $E^{\rm max}_{\Delta R=0.25}$ cut that would adequately reduce the $t\bar{t}$-induced background to an acceptable level. Until full Monte Carlo simulations of lepton isolation in energetic b-jet decay (that include the requirement that the lepton has a very large fraction of the b momentum) are performed, the effective value of A will not be known. Nor will it be known if non-gaussian tails arise. However, we are optimistic that the appropriate A value will not turn out to be significantly larger than $A = 0.5$, and will lie below $A = 1$. In the ensuing plots and discussion, we will consider $A = 0.5$.

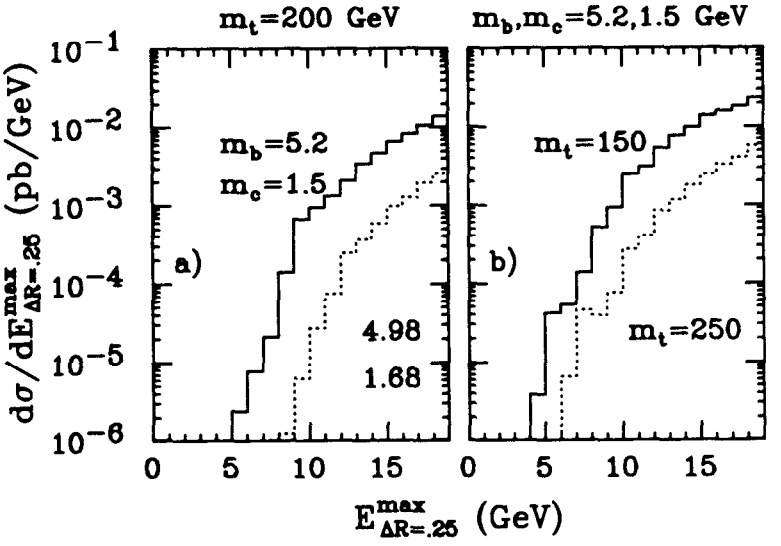

Figure 3: $t\bar{t}$ background $E^{\rm max}_{\Delta R=0.25}$ distributions computed for a variety of mass choices. In a) we compare $m_t = 200$ GeV results for the $m_b = 5.2, m_c = 1.5$ GeV and $m_b = 4.98, m_c = 1.68$ GeV mass choices. In b) we present results for $m_t = 150$ and 250 GeV, for $m_b = 5.2, m_c = 1.5$ GeV. We take $\sqrt{s} = 40$ TeV and employ the cuts of Eqs. (3) with the added requirement of $p_T^{\rm max,5} < 125$ GeV. Energetic jet cuts and jet tagging are not imposed. Branching fractions for $W^+ \to l^+\nu$ are not included. Resolution smearing using $A = 0.5$ is included in all cases.

In Fig. 3 we plot $E^{\rm max}_{\Delta R=0.25}$ distributions for the $t\bar{t}$ background in several other

$A = 0.5$ cases. First, in a) we compare $m_t = 200$ GeV results for the $m_b = 5.2, m_c = 1.5$ GeV and $m_b = 4.98, m_c = 1.68$ GeV mass choices — as discussed earlier, the latter are designed to conform to a more realistic fit of the lepton spectrum in B meson decay. We see that the $t\bar{t}$ background can be eliminated by an even less restrictive $E^{\rm max}_{\Delta R=0.25}$ cut in the case of the latter masses. This is easily understood. Since m_c/m_b is larger for these latter mass choices, the fraction of energy carried by the hadronic charm jet in $\bar{b}$ decay is larger than for the 5.2, 1.5 GeV mass choices. An l^+ of given energy from $\bar{b}$ decay thus has a significantly more energetic associated charm jet on average. We have also explored the effectiveness of an $E^{\rm max}_{\Delta R=0.25}$ cut for lower and higher m_t values. Results at $m_t = 150$ GeV and $m_t = 250$ GeV are given in part b) of Fig. 3, for our more conservative b, c mass choice, $m_b = 5.2, m_c = 1.5$ GeV. Lower top quark masses (in this range) cause the $E^{\rm max}_{\Delta R=0.25}$ distribution to extend to slightly lower values, but it appears that one can still find a cut significantly above the 1.5 GeV minimum-bias/pileup level that will effectively eliminate the $t\bar{t}$ background. Finally, we have not plotted the $p_T^g \geq 30$ GeV $t\bar{t}g$ background in these comparisons since, as found earlier, its $E^{\rm max}_{\Delta R=0.25}$ distributions do not extend any lower than the $E^{\rm max}_{\Delta R=0.25}$ distributions plotted for the $t\bar{t}$ background.

Summary of SSC Results

To summarize, it is clear that the $M^{\rm min}_{jl}$ and $E^{\rm max}_{\Delta R=0.25}$ procedures are quite comparable in the end. Although, as seen by comparing the last two rows of Table 1, the purely electroweak S/B ratio for the W^+W^+ pair processes is not quite as favorable when no $M^{\rm min}_{jl}$ cut is employed, the $t\bar{t}$-induced backgrounds must be included in a full comparison. In terms of yearly ($L = 10$ fb^{-1}) SSC event rates one obtains $S = 8.4$, $B = 3.5$, g-exchange= .6, and $t\bar{t}+t\bar{t}g \sim 0$ in the $E^{\rm max}_{\Delta R=0.25} < 8$ GeV cut procedure (for $A = 0.5$). This yields a net signal to combined-background ratio of $8.4/4.1 \simeq 2$. Some improvement in this ratio is possible if the $p_T^{\rm max,2} < 70$ GeV cut (discussed in Ref. [5]) is implemented, but 1 signal event (per SSC year) is lost. In comparison, the $M^{\rm min}_{jl}$ procedure yields $S = 6.4$, $B = 1.9$, g-exchange~ 0.1, $t\bar{t} + t\bar{t}g \simeq 1.3$, or a net signal to combined-background ratio of $6.4/3.2 \simeq 2$. Thus, the signal to background ratios obtained via the two procedures are very similar, but we see that the $E^{\rm max}_{\Delta R=0.25}$ cut does retain about 2 more signal events than does the $M^{\rm min}_{jl}$ cut.

In neither case, however, does the statistical significance of the signal, computed as[⋆]

$$N_{SD} = \frac{S}{\sqrt{S + B + g\text{−exchange} + t\bar{t} + t\bar{t}g}}, \tag{8}$$

⋆ Since the backgrounds will be very difficult to independently normalize, this is the only appropriate estimate of statistical significance.

exceed $N_{SD} = 2.5$. Thus, detection of the like-sign signal at the SSC in one canonical year would not appear to be possible. A 4σ effect in the l^+l^+ channel requires about $L = 40$ fb^{-1} of integrated luminosity using the $M_{jl}^{\rm min}$ cut procedure, and about $L = 30$ fb^{-1} using the $E_{\Delta R=0.25}^{\rm max}$ technique. The l^-l^- channel yields about 1/3 as many S, B, and g-exchange events as does the l^+l^+ channel, whereas the $t\bar{t}$ and $t\bar{t}g$ backgrounds yield equal numbers of l^-l^- and l^+l^+ events. Summing the l^+l^+ and l^-l^- channels, we find that the integrated luminosities required for $N_{SD} = 4$ are 30 fb^{-1} and 20 fb^{-1} for the $M_{jl}^{\rm min}$ and $E_{\Delta R=0.25}^{\rm max}$ procedures, respectively.

The signal to background ratio may actually be improved, with relatively small sacrifice of signal, by choosing a rapidity cut on the leptons of $|y_l| < 2.5$, rather than the 3.5 employed in our tables. For example, after the $E_{\Delta R=0.25}^{\rm max}$ cut procedure we obtain $S = 16$ fb and $B = 5.6$ fb in place of the $S = 17$ fb and $B = 7.1$ fb appearing in Table 1 (recall that $W^+ \to l^+\nu$ branching ratios are not included in these cross sections). (The g-exchange cross section exhibits a percentage decrease intermediate between that found for S and B.) However, it turns out that the integrated luminosity required to achieve $N_{SD} = 4$ is almost identical for the $|y_l| \leq 3.5$ and $|y_l| \leq 2.5$ cuts. Certainly, further decreasing the $|y_l|$ cut does not appear to be useful. First, it leads to significant loss of signal rate. Moreover, our results show that after the $M_{jl}^{\rm min}$ cut the B background actually decreases less rapidly than the signal as the rapidity cut is narrowed below 2.5. If the isolation cut is employed, all of the backgrounds do continue to decrease slightly more rapidly than the signal S, but, at a given integrated luminosity, N_{SD} is always worse for a rapidity cut less than 2.5 than for a rapidity cut between 2.5 and 3.5. For instance, because of the loss of signal events for a $|y_l| \leq 1.5$ cut, to achieve $N_{SD} \geq 4$ after combining the l^+l^+ and l^-l^- channels would require about $L = 40$ fb^{-1} if the isolation cut is employed.

4. Sensitivity of SSC Results to Distribution Functions and Scale Choice

In this section, we present numerical results in the format of Table 1 for the signal S, background B, and gluon exchange, for three alternative distribution function and momentum transfer scale choices:

1. HMRS(B) distributions and the momentum transfer scale choice of Ref. [6] specified in Eq. (1);
2. EHLQ ($\Lambda_{QCD} = 0.29$ GeV) distribution functions and our standard momentum transfer scale choice, $Q^2 = \hat{s}$;
3. EHLQ distributions and Q^2 as in Eq. (1).

The results for these three choices are indicated in order in Table 2, following the format of Table 1. Other possible distribution function choices, for which we do not give explicit numerical results, include the HMRS(E) set obtained by the

HMRS collaboration from a fit employing EMC data, which yields results somewhat smaller than those for the HMRS(B) set, and the Duke-Owens distribution functions (employed in our earlier work, Ref. [5]) that yield signal and background cross sections that are quite similar to those obtained for the HMRS(B) set.

Cut	S	B	g-exch.
$M_{ll} > 300$, $\|y_l\| < 3.5$, $p_T^l > 75$	23,22,25	105,75,92	28,26,28
	(23,22,24)	(99,70,86)	(19,19,19)
$z_{ll} \leq -0.8$, $\delta p_T^{ll} \geq 200$	19,22,23	52,36,43	13,12,13
	(23,22,23)	(45,32,39)	(7.2,7.4,7.4)
$p_T^{\max,5} \leq 125$	11,14,16	14,6.7,7.7	1.2,1.5,1.5
	(11,14,16)	(14,6.4,7.5)	(0.99,1.2,1.2)
$p_T^{\max,5} \leq 125$, $M_{jl}^{\min} \geq 200$	(7.4,11,13)	(11,3.4,4.3)	(.11,.11,.12)
$p_T^{\max,5} \leq 125$, $E_{\Delta R=0.25}^{\max} < 8$	11,14,16	14,6.6,7.6	1.2,1.4,1.4

Table 2: We give the electroweak cross sections in femtobarns for the signal, S, the $\mathcal{O}(\alpha_W^2)$ background, B, and for the $\mathcal{O}(\alpha_W \alpha_s)$ g-exchange background, after imposing various cuts. The format and definitions for this table are exactly as for Table 1. The triplets of numbers correspond to the three different distribution function and scale choices delineated in the text in the order given there. $A = 0.5$ is employed for the $E_{\Delta R=0.25}^{\max}$ cut results.

Table 2 shows that there are differences between the results obtained using different distribution functions and momentum transfer scale choices. For EHLQ distribution functions and either $Q^2 = \hat{s}$ or Q^2 as given in Eq. (1) (the 2nd and 3rd numbers in the triplets of Table 2), the overall levels of the signal and irreducible W^+W^+ backgrounds after various cuts are quite comparable to those obtained in Table 1 of the previous section for the HMRS(B) distributions and $Q^2 = \hat{s}$. However, for HMRS(B) structure functions and Q^2 of Eq. (1) (the 1st number in the triplets), the background remaining after cuts is significantly larger than for the other three cases, while the signal is significantly smaller — smaller, in fact, than the background. This is, of course, related to the detailed way in which the HMRS(B) distributions change as a function of Q^2 in the relevant range of x. The different behavior of signal and background as the choice for Q^2 is varied between $\hat{s}$ and Eq. (1) is a result of the fact that the $\hat{s}$ and spectator p_T values for the LL polarization component are significantly smaller than those for the background (which derives from transverse polarization modes). Clearly, computation of higher

order corrections to the subprocesses considered and improved knowledge of quark distribution functions (that will be forth coming from HERA) will both help to reduce the uncertainties illustrated in Table 2. For now, it is sufficient to note that all choices considered above predict a similar signal event rate, but that the background could be larger than for our standard choices of HMRS(B) distribution functions and $Q^2 = \hat{s}$. This would imply that somewhat larger integrated luminosity, than that estimated in the previous section, would be required to achieve $N_{SD} = 4$ at the SSC.

5. Signal and Background Results for the LHC and Eloisatron

It is, of course, of interest to know how our results change as the machine energy is altered. We have considered two machine energies in addition to that of the SSC: the LHC at $\sqrt{s} = 16$ TeV, and the Eloisatron with hypothetical energy of $\sqrt{s} = 200$ TeV. In Table 3 we give results for all three machine energies following the general format of Table 1, except that we quote event rates for an integrated luminosity of 10 fb^{-1} (the canonical yearly luminosity for an instantaneous luminosity of $\mathcal{L} = 10^{33}$ cm^{-2}sec^{-1}). We also omit the gluon-exchange and $t\bar{t}g$ backgrounds. We employ the same distribution functions and scale choice (HMRS(B) and $Q^2 = \hat{s}$) as in Table 1. Event rates are quoted in the order of increasing machine energy: LHC, SSC, Eloisatron.

These results indicate that the LHC will have great difficulty with this type of signal. For instance, after the $E^{\max}_{\Delta R=0.25} < 8$ GeV cut, the LHC yields only about 1 signal event per year vs. a background of about 0.6 events. Even if the accumulated luminosity is assumed to be a factor of ten larger, *i.e.* 100 fb^{-1}, detection of the like-sign signal for a 1 TeV SM Higgs boson appears hopeless. Indeed, the LHC at $L = 100$ fb^{-1} yields only a slightly larger value of N_{SD} (Eq. (8)) than does the SSC with $L = 10$ fb^{-1}. As stated earlier, we estimate that at least $L = 20$ fb^{-1} is required at the SSC for detection of the like-sign dilepton Standard Model 1 TeV Higgs signal, while at the LHC about 190 fb^{-1} would be required (where in both cases we assume that the $E^{\max}_{\Delta R=0.25}$ procedure is employed and we sum l^+l^+ and l^-l^- channels). Of course, the Eloisatron event rates for 10 fb^{-1} in the like-sign channel are even larger than for the SSC, *e.g.* by a factor of about 13 for both the signal and background after the $E^{\max}_{\Delta R=0.25} < 8$ GeV cut. Thus, the Eloisatron energy choice yields an increase of event rate that would be appropriate for a worthwhile successor to the SSC; it would be capable of accumulating enough events after several years of running to allow an actual measurement of the M_{ll} spectrum.

Cut	S	B	$t\bar{t}$
$M_{ll} > 300$, $\lvert y_l \rvert < 3.5$, $p_T^l > 75$	1.6,12,180	5.6,46,550	1000,10000,1.6×10^5
	(1.6,12,170)	(5.2,43,540)	(83,660,8300)
$z_{ll} \leq -0.8$, $\delta p_T^{ll} \geq 200$	1.5,11,150	2.8,21,250	870,8900,1.4×10^5
	(1.4,11,150)	(2.6,19,240)	(58,470,5800)
$p_T^{\max,5} \leq 125$	1.1,8.2,110	0.65,3.5,44	410,3300,42000
	(1.1,8.2,110)	(0.63,3.4,44)	(42,330,3500)
$p_T^{\max,5} \leq 125$, $M_{jl}^{\min} \geq 200$	(0.83,6.5,73)	(0.29,1.9,26)	(0.062,0.42,6.3)
$p_T^{\max,5} \leq 125$, $E_{\Delta R=0.25}^{\max} < 8$	1.1,8.2,110	0.65,3.5,44	0.01,0.016,0.19

Table 3: We give the event rates for integrated luminosity of $L = 10$ fb^{-1} for the electroweak signal, S, the $\mathcal{O}(\alpha_W^2)$ background, B, and the $t\bar{t}$ background, after imposing various cuts. The format and cut definitions for this table are as in Table 1. Only the l^+l^+ event rates are given here. The triplets of numbers correspond to the LHC, SSC and Eloisatron machine energy choices, respectively. HMRS(B) distributions with $Q^2 = \hat{s}$ are employed. Branching ratios for the $W^+ \to l^+\nu$ decays *are* included in this table. The W^-W^- final state yields about 1/3 as many S and B events in the l^-l^- channel as the number of l^+l^+ events listed in this table. The $t\bar{t}$ background event rate is the same in the l^-l^- channel as in the l^+l^+ channel. $A = 0.5$ is employed for the $E_{\Delta R=0.25}^{\max}$ cut results.

6. Discussion and Conclusions

We conclude with a variety of remarks. First, we emphasize that either our originally proposed $M_{jl}^{\min}$ cut procedure or an isolation cut can be effectively employed to eliminate $t\bar{t}$-induced backgrounds to the like-sign dilepton signal for the strong scattering of longitudinally polarized W^+'s, as conservatively typified by the SM for a Higgs mass of 1 TeV. The principal remaining concern is simply that of event rate. In the l^+l^+ channel, something like 6.5 to 8.5 (depending upon whether $M_{jl}^{\min}$ or isolation is employed) signal (S) events per SSC year (and about one-third this many in the l^-l^- channel) survive the cuts for $L = 10$ fb^{-1}. It is clear that running at higher luminosity in order to enhance the event rate would be highly desirable. To obtain a statistical significance of $N_{SD} = 4$ we have estimated in Sec. 3 that about $L = 30$ fb^{-1} or $L = 20$ fb^{-1} accumulated luminosity is required, for the $M_{jl}^{\min}$ and $E_{\Delta R=0.25}^{\max}$ procedures respectively, if l^+l^+ and l^-l^- events are summed. The $M_{jl}^{\min}$ cut procedure should be quite robust against the effects of pileup because of the energetic jet tag involved. The lepton isolation cut must be

approached a bit more cautiously, as pileup events might create a significant tail at large $E^{\rm max}_{\Delta R=0.25}$ for the signal events — events in this tail would then be lost if a stringent $E^{\rm max}_{\Delta R=0.25}$ cut is imposed. Other concerns include the true efficiency of the $M^{\rm min}_{jl}$ cut for the signal events, and the appropriate resolution/hadronization smearing for the charm quark jet in the $E^{\rm max}_{\Delta R=0.25}$ procedure. We are optimistic that a full detector simulation and Monte Carlo study which includes initial state radiation and hadronization will justify our expectations that the $M^{\rm min}_{jl}$ cut will remain highly efficient for signal events, and that the effective smearing resolution will not be dramatically worse than the basic $50\%/\sqrt{E}$ resolution typically expected for an SSC detector.

Second, concerning backgrounds, we remark that there is an additional background that we have not computed, but that we believe should be eliminated by precisely the same cuts that we have discussed for the $t\bar{t}$-induced background. The process is $qg \to qt\bar{b}$ (to which graphs involving $W^+g \to t\bar{b}$ subgraphs contribute, for instance), followed by $t \to W^+b$ and $\bar{b} \to \bar{c}l^+\nu$. The uncut cross section for this process becomes comparable to that for $gg \to t\bar{t}$ for top quark masses somewhat above 200 GeV. The full sequence of cuts considered here should be very effective in suppressing this background. In particular, the W^+g fusion graphs produce a spectator quark that is similar in kinematic distribution to the spectator quarks for the g-exchange and pure electroweak W^+W^+ backgrounds, and thus they will be strongly suppressed already by the $p_T^{\rm max,5} < 125$ GeV cut. A further $E^{\rm max}_{\Delta R=0.25}$ cut should be just as effective in discriminating against the $\bar{b}$ semi-leptonic virtual decay as in the $t\bar{t}$ case studied in this paper. The $M^{\rm min}_{jl}$ cut requires a bit of discussion in view of the fact that the spectator quark of this new background can combine with one of the l^+'s to yield fairly large M_{jl} values. However, along with the $M^{\rm min}_{jl}$ cut we always impose as well the $n_j < 3$ cut, see Eq. (4). An event in which a large M_{jl} value is possible because the spectator jet is visible has a high probability of having $n_j = 3$, since in general the the b and $\bar{c}$ jets will also be visible. Thus, we believe that the $M^{\rm min}_{jl}$ cut in combination with the energetic jet cuts of Eq. (4) will be highly effective in eliminating this additional background, especially in view of the fact that it will already be suppressed by the $p_T^{\rm max,5}$ cut.

Another important point concerns the possibility that a light Higgs boson is found at the SSC or, earlier, at LEP or LEP-200. If this were to occur, an important goal at the SSC would be the measurement of the W^+W^+ scattering amplitude in the TeV region via the l^+l^+ signal as a check of Standard Model predictions. One of the best ways to test the SM prediction for this channel if m_{ϕ^0} is small will be to sequentially impose certain of the cuts discussed here. It turns out, as discussed below, that we can eliminate the $t\bar{t}+t\bar{t}g$ background *ab initio* by always demanding $E^{\rm max}_{\Delta R=0.25} \leq 8$ GeV. In order to keep the efficiency as high as possible, we will not impose the energetic jet cuts of Eq. (4) nor the $M^{\rm min}_{jl}$ cut. Then, to be certain of probing the TeV region, we require our first level leptonic cuts, $M_{ll} \geq 300$ GeV, $|y_l| \leq 3.5$ and $p_T^l \geq 75$ GeV. We next apply the $z_{ll}, \delta p_T^{ll}$ and $p_T^{\rm max,5}$

cuts in turn. Conformity to Standard Model predictions would consist of finding that S is negligible at *all* cut levels, *i.e.* that the event rate decreases according to the predictions for B+g-exchange. Any deviation from SM expectations would most likely appear as a deviation upon imposition of the $p_T^{\max,5}$ cut.

In more detail, the predictions are the following. As stated above, we will not impose either the cuts of Eq. (4) or the $M_{jl}^{\min}$ cut, but will impose the isolation cut from the beginning. It turns out that the (non-parenthetical) B, and g-exchange cross sections in the first two rows of Table 1 are essentially unaltered by the addition of the isolation cut, whereas the sum of the $t\bar{t}$ and $t\bar{t}g$ cross sections is $\lesssim 1$ fb and 0.2 fb for the first two rows, respectively. (The results for B, g-exchange and $t\bar{t}, t\bar{t}g$ after the isolation cut and after imposing the $z_{ll}, \delta p_T^{ll}$ and $p_T^{\max,5}$ cuts are already given in the last row of Table 1.) From these results, it is apparent that at all cut levels the $t\bar{t}$-induced backgrounds are negligible compared to $B+g$-exchange once $E_{\Delta R=0.25}^{\max} \leq 8$ GeV is required. In terms of the number of l^+l^+ events per $L = 10$ fb^{-1} SSC year, for small m_{ϕ^0} we would predict 60, 28 and 4.1 as we sequentially imposed a) the $M_{ll}, |y_l|, p_T^L$, b) the $z_{ll}, \delta p_T^{ll}$, and c) the $p_T^{\max,5}$ cuts, respectively. This makes it clear that with perhaps $L = 40$ fb^{-1} we could fully test the SM expectations for the l^+l^+ signal by comparing to the predictions for all three cut levels.

As a fourth, and very important observation, it should be emphasized that the procedures discussed here for enhancing signal over background in the W^+W^+ like-sign dilepton channel are almost certainly equally powerful for isolating the longitudinal-longitudinal signal in the purely leptonic final state modes of the resonating channels, W^+W^- and ZZ, not to mention the $W^\pm Z$ non-resonating channels. First, we note that the $p_T^{\max,5}$ cut, along with the lepton cuts, will be just as effective in eliminating the transverse polarization mode $qq \to qq + W^+W^-, ZZ, W^\pm Z$ backgrounds as in the W^+W^+ case studied here. Thus, since the $p_T^{\max,5}$ cut is highly efficient for the longitudinal mode signal of interest, one should certainly employ it for all these channels. There are, however, two important differences between the $W^+W^-, ZZ, W^\pm Z$ cases and the W^+W^+ channel discussed here. We outline these in turn below, explaining why our $M_{jl}^{\min}$ cut procedure remains highly effective.

The first distinction is that there are $q\bar{q}, gg \to W^+W^-, ZZ, W^\pm Z$ backgrounds for these other channels. Since at the lowest order in α_s at which these latter processes occur there is no extra jet in the final state, the $p_T^{\max,5}$ cut will not help to eliminate such backgrounds. However, the $M_{jl}^{\min}$ cut, which according to our study retains a large portion of the signal, and further suppresses the transverse mode backgrounds, will be highly effective in eliminating the $q\bar{q}, gg \to W^+W^-, ZZ$ backgrounds. Simply tagging a jet in order to construct $M_{jl}^{\min}$ already implies that these backgrounds must be computed at a higher order in α_s, and will be strongly suppressed by such a tag. Further, we would anticipate that the typical

$M_{jl}^{\rm min}$ value obtained at such higher order would not be large enough to pass the $M_{jl}^{\rm min} > 200$ GeV cut.

The second important difference concerns the $t\bar{t}$-induced backgrounds. These are negligible for the ZZ and $W^{\pm}Z$ cases, where a tight constraint on the mass of the l^+l^- pair from one or both Z's can be imposed. In contrast, the $t\bar{t}$ backgrounds are big for the W^+W^- channel. However, once again, the $M_{jl}^{\rm min}$ cut will be a very powerful means of eliminating these backgrounds. Since the opposite-sign leptons of interest from the t decays are energetic primary ones from the W decay products of the t's, they will almost certainly combine with the b jets to yield $M_{jl}^{\rm min} < m_t$, even after jet energy smearing and coalescence. And, we have seen that the extra gluon in the $t\bar{t}g$ final state does not create a significant tail with $M_{jl}^{\rm min} > m_t$. (Of course, we should note that an isolation cut is *not* effective in eliminating the $t\bar{t}$ induced backgrounds for this channel; nor is at all useful for eliminating the $q\bar{q} \to W^+W^-, ZZ, W^{\pm}Z$ processes.) Overall, it seems clear that the lepton, anti-tagging $p_T^{\rm max,5}$ and $M_{jl}^{\rm min}$ cuts employed here for our W^+W^+ study are very likely to yield viable signals for the purely leptonic modes of the W^+W^-, ZZ and $W^{\pm}Z$ channels, for a SM Higgs with mass in the 1 TeV range.

Finally, we note that the Standard Model $m_{\phi^0} = 1$ TeV event rates found in our study are significantly smaller than would be obtained in many of the more general models of a strongly-interacting vector boson sector.[16] For $L = 10$ fb^{-1}, the signal rates predicted by such models would generally be highly visible after either of our cut sequences. In particular, it seems relatively certain that the efficiency of the $p_T^{\rm max,5}$ cut for the signal cross sections in these other models, although not necessarily exactly the same as that found in the case of the SM Higgs signal, would still be very high. Thus, our results lead to considerable optimism that the scattering of longitudinally polarized W^+'s and W^-'s will be detectable at the SSC via the observation of like-sign dilepton pairs.

Acknowledgements

We would like to thank R.M. Barnett, M. Chanowitz, V. Barger, T. Han, F. Paige, M. Peskin, W.J. Stirling and S. Stone for helpful discussions and communications. Computing resources were provided by the University of Texas Center for High Performance Computing. This research was supported in part by the U.S. Department of Energy under Contracts No. DE-FG05-85ER40200, No. DE-AT03-89ER40492 and No. DE-AC03-76SF00515.

REFERENCES

1. M.S. Chanowitz and M.K. Gaillard, *Nucl. Phys.* **B261** (1985) 379.
2. M.S. Chanowitz and M. Golden, *Phys. Rev. Lett.* **61** (1988) 1053, and Erratum, *Phys. Rev. Lett.* **63** (1989) 446.
3. R. Vega and D.A. Dicus, *Nucl. Phys.* **B329** (1990) 533.
4. V. Barger, K. Cheung, T. Han, and R.J.N. Phillips, *Phys. Rev.* **D42** (1990) 3052.
5. D. Dicus, J.F. Gunion and R. Vega, *Phys. Lett.* **258B** (1991) 475.
6. M. Berger and M. Chanowitz, LBL-30476 (1991).
7. P.N. Harriman, A.D. Martin, W.J. Stirling, and R.G. Roberts, *Phys. Rev.* **D42** (1990) 798.
8. E. Eichten, I. Hinchliffe, K. Lane, and C. Quigg, *Rev. Mod. Phys.* **56** (1984) 579. Updated versions for $\Lambda_{\overline{MS}} = 0.29$ GeV have been provided by I. Hinchliffe and R.M. Barnett.
9. U. Amaldi *et al.*, *Nucl. Phys.* **B297** (1988) 244; D. Haidt, in *Weak Interactions in Neutrinos,* Proceedings of the 12th International Workshop, Ginosar, Israel, 1989, eds. P. Singer and B. Gad Eilan [*Nucl. Phys. Proc. Suppl.* **B13** (1990)]; J. Ellis and G. Fogli, *Phys. Lett.* **249B** (1990) 543; V. Barger, J.L. Hewett, T. Rizzo, *Phys. Rev. Lett.* **65** (1990) 1313.
10. S. Stone, private communication.
11. G. Altarelli *et al.*, *Nucl. Phys.* **B208** (1982) 365.
12. J.F. Gunion and Z. Kunszt, *Phys. Lett.* **178B** (1986) 296; R.K. Ellis and J.C. Sexton, *Nucl. Phys.* **B282** (1987) 642.
13. We have benefitted from conversations with M. Felcini, G. Forden, A. Nisati and E. Wang in regard to the ensuing smearing discussion.
14. The SDC Collaboration (G. Trilling *et al.*), Letter of Intent, SSCL-SR-1153A, SDC-90-00151 (1990).
15. We thank F. Paige for this estimate.
16. See, for example, the comparisons in Refs. [4] and [6].